Original Article

Computational Survey of FHIT, A Putative Human Tumor Suppressor, Truncates Structure

Ameneh Eslamparast [1], Mohammad Hossein Ghahremani [2], and Soroush Sardari [3*]

1. Biotechnology Research Center, Pasteur Institute of Iran, Tehran, Iran
2. Department of Pharmacology-Toxicology, Faculty of Pharmacy, Tehran University of Medical Sciences, Tehran, Iran
3. Drug Design and Bioinformatics Unit, Medical Biotechnology Department, Biotechnology Research Center, Pasteur Institute of Iran, Tehran, Iran

Abstract

Background: Fragile Histidine Triad protein (FHIT), as a known tumor suppressor protein, has been proposed to play crucial role in inhibiting p53 degradation by MDM2. Studies have confirmed FHIT interaction with p53 or MDM2, although functional interacting domains of FHIT with MDM2 and/or p53 are not completely defined. Thus, through determining the significant structural interacting domains of FHIT, information with regard to MDM2 and p53 would be provided. As there were no previous studies evaluating the interaction of optimized important parts of target molecules, docking study was employed.

Methods: Truncated structures of FHIT were screened to reveal critical sections engaging in FHIT interaction. HEX program was used in order to study the interaction of target structures.

Results: Given the total energy, FHIT structures (β5-7, α1) and (α1) of FHIT were showed to be better candidates in comparison with other structures in interaction with optimized MDM2 part. Furthermore, FHIT structures (β4-7, α1) and (β5-7, α1) were considered to be better than other structures in interaction with optimized p53 part. FHIT truncates which interact with MDM2 optimized part exhibited lower energy levels than FHIT truncates which interact with p53 optimized part.

Conclusion: Our results can be useful for designing new inhibitors of this protein complex interaction which would result in tumor repression.

Avicenna J Med Biotech 2014; 6(2): 64-71

Keywords: Fragile histidine triad protein, MDM2 protein, Tumor suppressor proteins

*** Corresponding author:**
Soroush Sardari, Ph.D.,
Drug Design and Bioinformatics Unit, Medical Biotechnology Department, Biotechnology Research Center, Pasteur Institute of Iran, Tehran, Iran
Tel: +98 21 66405535
Fax: +98 21 66465132
E-mail:
ssardari@hotmail.com;
sardari@pasteur.ac.ir
Received: 5 Oct 2013
Accepted: 15 Dec 2013

Introduction

FHIT belongs to Histidine Triad (HIT) nucleotide-binding protein superfamily and is considered a tumor suppressor [1]. Genomic alterations and aberrant expression of FHIT have been correlated with many types of human cancers, including those of the lung [2-4], breast [5,6], cervix [7], colon [8], pancreas [9], prostate [10], stomach [11,12], head and neck [13].

Studies have shown the interaction of FHIT with MDM2 and the block of the interaction of MDM2 with p53, result in increased stability of p53 [14]. Structurally, FHIT forms a dimer in solution (PDB code: 1FIT) and general structure of its protomer can be described as a common α+β type [15]. An ordinary hydrophobic core is formed within the background of

the dimer [16].

As prior studies demonstrate, MDM2 protein interacts with p53 directly [17,18] and MDM2 can interact with FHIT (by immunoprecipitation) [14]. Moreover, other studies confirm the interaction of p53 and FHIT [14,19]. Thus, it is logical to consider that FHIT and p53 have binding sites on MDM2 and perhaps these proteins could influence each other in binding to MDM2.

As functional interacting domains of FHIT with MDM2 and/or p53 are not completely defined, therefore, by exploring the recognition site of interaction of FHIT-MDM2 with regard to p53 binding, one can evaluate the interaction and/or competition amid these proteins for therapeutical approaches. Furthermore, the research for functional domain of FHIT may reveal the protein domain responsible for tumor suppression. In addition, these studies will shed lights on the molecular mechanism of FHIT-MDM2-p53 complex.

In this study, we assessed FHIT constructs interaction with MDM2 and p53 optimized models *in silico*. Results can be useful for designing new inhibitors of this protein complex interaction which would result in tumor repression.

Materials and Methods

Tertiary structure determination of FHIT truncates

PDB file of FHIT consisted of residues 2-106 and 127-147, was achieved from protein databank (PDB code: 1FIT). Based on previous studies, fourteen segmented structures were constructed by truncating pdb file using ViewerLite42 (2010).

PDB file of MDM2 and p53 optimized truncates, consisted of amino acids 23-119 of MDM2 and 18-26 of p53, were achieved from protein databank (PDB code: 1T4F) with using ViewrLite42.

FHIT, MDM2 and p53 modeling

The structure prediction process consisted of sequence alignment, model building, and structure refinement stages [20].

The tertiary structure of full FHIT was established by homology modeling using the pdb three dimensional structure of FHIT, available from the protein databank (1FIT) as template by Swiss homology modeling server, and Modeller 9v7 (2009) package (Table 1) [21].

Homology modeling was used to achieve the complete models of MDM2 and p53. Swiss homology modeling server and I-TASSER server were used for modeling the gaps of

Table 1. FHIT truncated structures

		FHIT β strands and α helices from N-terminal to C-terminal		
Structure no.	**Amino acids**	**N-terminal**	**C-terminal**	
1	(2-147) full FHIT	β1, β2, β3, β4, β5	α1	β6, β7 α2
2	(2-12)	β1, β2	--	--
3	(2-43)	β1, β2, β3, β4	--	--
4	(2-50)	β1, β2, β3, β4, β5	--	--
5	(17-102)	β3, β4, β5	α1	β6, β7
6	(21-104)	β4, β5	α1	β6, β7
7	(22-102)	β4, β5	α1	β6, β7
8	(22-106)	β4, β5	α1	β6, β7
9	(34-106)	--	α1	β6, β7
9b *	(34-102)	--	α1	β6, β7
10	(51-106)	--	α1	β6, β7
10b *	(51-102)	--	α1	β6, β7
11	(53-73)	--	α1	--
12	(75-106)	β5	--	β6, β7
12b *	(75-102)	β5	--	β6, β7

* Note: C9b, C10b, C12b were created by truncating 4 amino acids from the end point of each constructs

MDM2 and p53. Connecting MDM2 and p53 five segments was performed by means of Modeller 9v7 program. Ramachandran plot generated by spdb viewer was used to assess the best models of each molecule. Nominees were evaluated using PROCHECK. Energy minimization of the obtained structures was performed using Swiss-Pdb Viewer 4.01 (2010).

Computational interaction studies

Docked conformations and interaction energies were achieved using the protein-protein docking package HEX 5.1 (2008). During docking operation by HEX, the free energies were estimated based on shape complementarity only and shape/electrostatics. The mean computational time used for a complex was about 30 *min* for HEX. HEX was executed on an IBM attuned computer running at 4 *GB* RAM and 2.5 *GHz* Dual Core™2 Intel® CPU.

Results

Determination and generation of FHIT truncated structures

As mentioned before, we created 14 different truncated structures (Table 1), namely 2 to 12b and compared them with full length FHIT (Structure 1, Table 1) to recognize the most critical regions of FHIT involved in the interaction with MDM2 and p53 and also evaluate trimeric interaction complex. Tertiary structures of MDM2 and p53 optimized truncates, composed of amino acids 23-119 and 18-26, were obtained from protein databank (PDB code: 1T4F) (Figure 1).

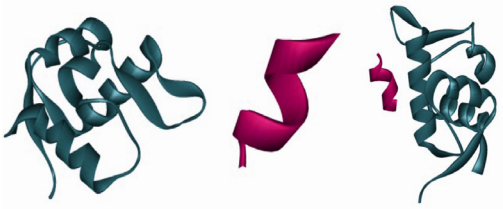

Figure 1. MDM2 optimized part (left), p53 optimized part (between) and 1T4F (PDB file) (right)

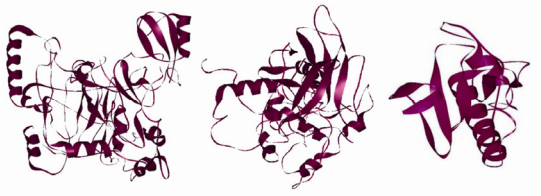

Figure 2. MDM2 complete model (left), p53 complete model (between) and FHIT complete model (right)

Complete FHIT, MDM2 and p53 models

FHIT (Structure 1, Table 1), MDM2 and p53 structures were generated by homology modeling (Figure 2).

Interaction analysis

HEX results: The docking results performed by HEX for FHIT truncates with complete MDM2 and MDM2 optimized part, p53 optimized part are shown in tables 2-4.

Table 2. Docking interaction energies (*kJ/mol*) of FHIT truncates with MDM2 and p53 optimized part

Target: FHIT constructs	β strands	α helices	E-total (MDM2 optimized part)	E-total (p53 optimized part)
1 (Full length)	β1-7	α1-2	-426.58	-325.53
2 (2-12)	β1-2	--	-357.46	-227.31
3 (2-43)	β1-4	--	-425.62	-309.70
4 (2-50)	β1-5	--	-459.68	-324.75
5 (17-102)	β3-7	α1	-460.98	-358.14
6 (21-104)	β4-7	α1	-462.99	-374.86
7 (22-102)	β4-7	α1	-434.99	-321.44
8 (22-106)	β4-7	α1	-456.14	-345.26
9 (34-106)	β5-7	α1	-487.87	-365.59
9b (34-102)	β5-7	α1	-479.24	-331.74
10 (51-106)	β6-7	α1	-456.22	-347.92
10b (51-102)	β6-7	α1	-457.84	-344.99
11 (53-73)	--	α1	-477.68	-275.81
12 (75-106)	β6-7	--	-423.27	-279.01
12b (75-102)	β6-7	--	-386.03	-289.22

Table 3. Docking interaction energies (*kJ/mol*) of FHIT truncates with MDM2 complete model

Target: FHIT truncates		β strands	α helices	E-total (MDM2 complete model)	E-shape (MDM2 complete model)
1	(Full length)	β1-7	α 1-2	-459.53	-514.69
2	(2-12)	β1-2	--	-470.78	-404.28
3	(2-43)	β1-4	--	-481.25	-459.89
4	(2-50)	β1-5	--	-564.96	-537.94
5	(17-102)	β3-7	α1	-526.42	-523.61
6	(21-104)	β4-7	α1	-519.84	-560.65
7	(22-102)	β4-7	α1	-523.92	-579.12
8	(22-106)	β4-7	α1	-458.58	-508.41
9	(34-106)	β5-7	α1	-501.87	-499.37
10	(51-106)	β6-7	α1	-474.26	-471.92
11	(53-73)	--	α1	-476.76	-420.12
12	(75-106)	β6-7	--	-451.34	-461.33

Table 4. Docking interaction energies (*kJ/mol*) of MDM2 optimized part with FHIT truncates, interaction of this complex with p53 optimized part, interaction of p53 optimized part with FHIT truncates, and interaction of this complex with MDM2 optimized part

Target: FHIT truncates		β strands	α helices	E-total (MDM2 optimized part)	E-total (MDM2 optimized part, p53 optimized part)	E-total (p53 optimized part)	E-total (p53 optimized part, MDM2 optimized part)
1	(Full length)	β1-7	α1-2	-426.58	-457.02	-325.53	-476.38
2	(2-12)	β1-2	--	-343.90	-308.59	-227.31	-480.43
3	(2-43)	β1-4	--	-425.62	-446.11	-309.70	-448.76
4	(2-50)	β1-5	--	-459.68	-447.22	-324.75	-441.16
5	(17-102)	β3-7	α1	-460.98	-443.05	-358.14	-482.89
6	(21-104)	β4-7	α1	-462.99	-440.05	-374.86	-452.90
7	(22-102)	β4-7	α1	-434.99	-419.11	-321.44	-472.99
8	(22-106)	β4-7	α1	-456.14	-372.62	-345.26	-447.14
9	(34-106)	β5-7	α1	-487.87	-352.35	-365.59	-472.57
9b	(34-102)	β5-7	α1	-479.24	-440.94	-331.74	-471.50
10	(51-106)	β6-7	α1	-456.22	-417.22	-347.92	-453.76
10b	(51-102)	β6-7	α1	-457.84	-411.13	-344.99	-484.31
11	(53-73)	--	α1	-477.68	-357.41	-275.81	-431.02
12	(75-106)	β6-7	--	-423.27	-430.00	-279.01	-428.81
12b	(75-102)	β6-7	--	-386.03	-436.80	-289.22	-438.68

In table 2, E-totals refer to the interaction of FHIT constructs with partial MDM2 of 1T4F (cut p53 optimized part) and p53 optimized part of 1T4F (deleted MDM2 part).

Table 5 indicates docking total energy of complete MDM2 and p53 as well as MDM2 optimized part and p53 optimized part.

Considering the shape and electrostatic energies, FHIT truncated forms 9 (β5-7, α1), 9b (β5-7, α1) and 11 (α1) interact with MDM2 optimized part at lower total energy and the interaction of FHIT with p53 optimized part is better for structures 6 (β4-7, α1), 9 (β5-7, α1) and 5 (β3-7, α1) based on total energy (Table 2).

Table 5 demonstrates total interaction energy of optimized part of MDM2 with optimized part of p53 obtained from PDB protein databank. Docking interaction energy of these two structures is -407.20 (*kJ/mol*). This table also shows total interaction energy of MDM2 complete model and p53 complete model (-399.25 *kJ/mol*).

As table 3 shows, truncated structures 7 (β4-7, α1), 6 (β4-7, α1) and 4 (β1-5) interact with MDM2 complete model with lower E-shape (shape energy). Truncated structures 4 (β1-5), 5 (β3-7, α1) and 7 (β4-7, α1) dock

Table 5. Docking interaction energies (*kJ/mol*) of MDM2 model with p53 model and optimized part of MDM2 with optimized part of p53

Receptor	Ligand	E-total
MDM2 (1-484)	p53 (1-392)	-399.25
MDM2 (Glu23-Val119)	p53 (Arg18-Leu26)	-407.20

MDM2 complete model (1-484) and optimized part (Glu23-Val119); p53 complete model (1-392) and optimized part (Arg18-Leu26)

with MDM2 complete model at lower total energy (shape and electrostatic energy) when compared to others. In general, structures in lower E-shape results have lower E-total (E-shape plus E-force) results.

Since there is a probability that FHIT and p53 might interact with MDM2 in a competitive way, we have also examined the interaction of triple protein complex FHIT, MDM2 optimized model and p53 optimized part in two stages. For this analysis, after interaction of FHIT constructs with optimized part of MDM2, these complexes (FHIT truncates with MDM2 optimized part) were tested with optimized part of p53. Similarly, following the interaction of FHIT truncates with optimized part of p53, the interaction of these complexes with optimized part of MDM2 was performed.

As table 4 illustrates, the complexes of truncates 2 (β1-2), 9 (β5-7, α1), 11 (α1) and

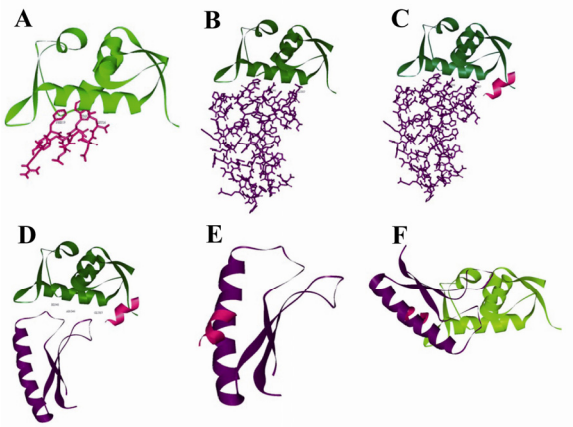

Figure 3. FHIT truncates, MDM2 optimized part, and p53 optimized part interactions three dimensional view. A) Three dimensional representation of 1T4F (PDB file); B) C9 FHIT truncate, MDM2 optimized part interaction view; C and D) C9 FHIT truncate and MDM2 optimized part interaction complex challenged with p53 optimized part; E) C9 FHIT truncate and p53 optimized part interaction view; F) C9 FHIT truncate and p53 optimized part interaction complex challenged with MDM2 optimized part

MDM2 optimized part interact with p53 optimized part in higher total energy status. On the other hand, complexes of p53 optimized part with truncates 12 (β6-7), 11 (α1) and 12b (β6-7) interact with MDM2 optimized part in a higher total energy circumstance. Figure 3 represents three dimensional view of some FHIT, MDM2 optimized part, and p53 optimized part interaction view. Figure 4 represents two dimensional view of C9 (FHIT34-

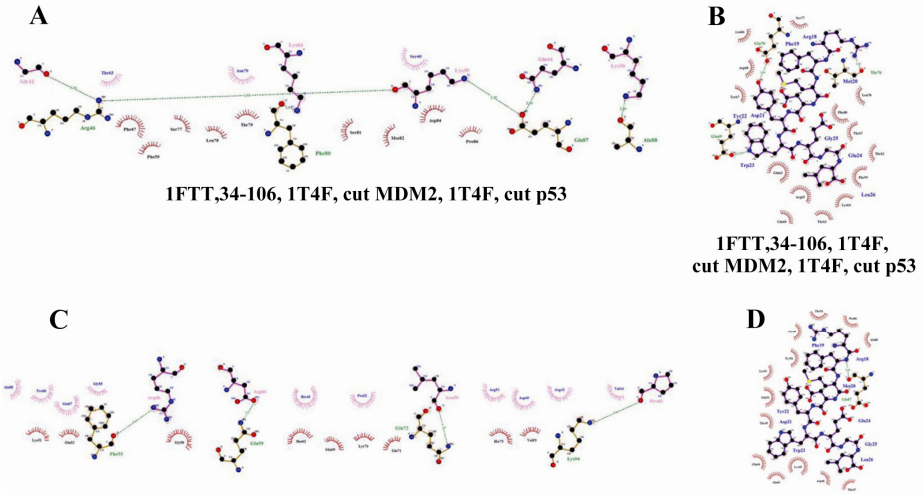

Figure 4. FHIT truncates, MDM2 optimized part, and p53 optimized part interactions, two dimensional view. A, B) C9 FHIT truncate and p53 optimized part interaction complex challenged with MDM2 optimized part; A) five residues of C9 involve in hydrogen bond in interaction with MDM2 optimized part, in this complex; B) p53 optimized part binding pocket. This binding pocket is composed of 17 residues in which three of them involve in hydrogen bond (Arg18, Asp21, and Trp23). C and D) C9 FHIT truncate and MDM2 optimized part interaction complex challenged with p53 optimized part; C) four residues of C9 involve in hydrogen bond in interaction with MDM2 optimized part, in this complex; D) p53 binding pocket. This binding pocket is composed of 14 residues in which one of them involve in hydrogen bond (Arg18)

106), MDM2 optimized part, and p53 optimized part important interactions view.

Discussion

Three dimensional structures of proteins are essential for computational interaction research. As only parts of FHIT, MDM2 and p53 had been determined as three dimensional structures in protein databank, we performed modeling for their structures.

Docking is considered as an *in silico* method for investigating the best interaction between two molecules which can be used in the rational drug design [22]. HEX program actually accelerates the process compared with the classical FFT docking algorithms [23]. Earlier studies have proved that HEX method has no limitation for protein size [24].

We tested docking of MDM2, p53 optimized parts as the receptor to compare the interaction tendencies of a special motif or a group of them within FHIT. The results of our previous docking study indicate that interaction of full FHIT with p53 (E-total: -568.66) and MDM2 (E-total: -459.53) is associated with lower total energy compared to the interaction of the complete MDM2 with p53 (E-total: -399.25). The abovementioned interaction occurred with higher total energy in comparison with the optimized p53 and MDM2 (E-total: -407.20). Moreover, subsequent to MDM2 and p53 optimization, it appeared that their relative tendency was augmented compared to their corresponding complete models.

Given the interaction of full FHIT with optimized models of p53 and MDM2, it is evident that FHIT truncates have higher affinity to interact with MDM2 optimized part than p53 optimized model. According to the interaction values, FHIT truncates interact with optimized MDM2 at lower E-total than optimized part of p53 and the total energies of docking interactions are directly related to shape energies of the mentioned interactions. Our results revealed that the tendency of β4-7, α1 segment of FHIT to p53 optimized model is more than other parts. Likewise, the β5-7, α1 structure of FHIT has more affinity to MDM2 optimized part than other forms. Thus, one can suggest the β5-7, α1 segment of FHIT as an interacting domain for both p53 and MDM2.

Having studied the above mentioned interactions, we found that FHIT remarkably has better affinity to bind MDM2 optimized part in the presence of p53 and MDM2 optimized models in most of the cases. Even though it can bind to p53 optimized model with low energy, when MDM2 optimized part is added to the model, the interaction with p53 optimized part is further attenuated (Table 4). Interestingly, complex of FHIT truncates interacting with MDM2 optimized part at lower total energy usually interacts with p53 optimized model at higher total energy. Thus, these findings indicate a sequence/conformation specificity of FHIT truncates for interacting with MDM2 or p53.

E-totals of interaction between MDM2 optimized model (for interaction with p53) and FHIT truncates reveal that α1 is important in these interactions. E-totals of interaction between p53 optimized model (for interaction with MDM2) and FHIT truncates show that β5-7 and α1 are important parts in these interactions.

Experimental reports using yeast two-hybrid [25] and immunoprecipitation indicate that p53 at amino acids 1-41 [25] or 1-52 [26] interacts with MDM2. On MDM2, the interaction at amino acids 1-118 [25] or 19-102 [26] is the binding site to p53. Site-directed mutagenesis confirms the Leu14, Phe19, Leu22, and Trp23 of p53 are essential amino acids for interaction [27]. The co-crystal structure of MDM2-p53 complex shows that Phe19, Trp23, and Leu26 are three main interacting residues in p53 [28].

MDM2 directly binds to p53 [18] and regulates p53 function and degradation [29-33]. Moreover, a number of studies reported p53 and FHIT interaction [14,19] and their possible association [34]. As shown in table 3, in p53-MDM2 interaction, the significant part of p53 is amino acids 18-26, and the important part of MDM2 is amino acids 23-119 [35]. Based on our results, the interaction sites of FHIT with

MDM2 and p53 have overlapping parts. The best interaction site for MDM2-FHIT is residues 34-106 containing β5-7, α1. Conversely, for FHIT-p53 interaction, amino acids 21-104 containing β4-7, α1 are involved. However, residues 34-104 are involved in both interactions (Table 2). Interestingly, when the interaction of FHIT with MDM2 optimized part is challenged with p53 optimized part, the interaction site is different from interaction with MDM2 optimized part alone.

Based upon these results, the interaction sites of FHIT with MDM2 and p53 are different with overlapping parts. FHIT binds to MDM2 with lower energy in the presence of p53 and the binding site shifts toward FHIT-MDM2 interaction. These data provide information involving competition of FHIT with p53 in binding to MDM2. Then, in the presence of FHIT, p53 is released from MDM2 and can increase apoptosis or cell cycle arrest. Figures 3 and 4 confirm the results indicated in the tables.

Conclusion

In conclusion**,** our findings provide valuable information to understand the molecular mechanism of FHIT-MDM2-p53 complex formation and the design of inhibitory compounds. The truncated parts of FHIT with higher absolute E-total energy interacting with MDM2 optimized part [parts (β5-7, α1) and/or (α1)] can be effective in inhibiting degradation of p53 through altering MDM2 interaction with p53. Also, the truncated parts of FHIT with higher absolute E-total energy interacting with p53 optimized part [parts (β5-7, α1) and (β4-7, α1)] can be effective in inhibiting degradation of p53 through altering MDM2 interaction site with p53.

Acknowledgement

This work was supported by Drug Design and Bioinformatics Unit, Pasteur Institute of Iran.

References

1. Croce CM, Sozzi G, Huebner K. Role of FHIT in human cancer. J Clin Oncol 1999;17(5):1618-1624.
2. Deng WG, Nishizaki M, Fang BL, Roth JA, Ji L. Induction of apoptosis by tumor suppressor FHIT via death receptor signaling pathway in human lung cancer cells. Biochem Biophys Res Commun 2007; 355(4):993-999.
3. Woenckhaus M, Merk J, Stoehr R, Schaeper F, Gaumann A, Wiebe K, et al. Prognostic value of FHIT, CTNNB1, and MUC1 expression in non-small cell lung cancer. Hum Pathol 2008;39(1): 126-136.
4. Kohno T, Yokota J. How many tumor suppressor genes are involved in human lung carcinogenesis? Carcinogenesis 1999;20(8):1403-1410.
5. Yang Q, Yoshimura G, Sakurai T, Kakudo K. The Fragile Histidine Triad gene and breast cancer. Med Sci Monit 2002;8(7):RA140-144.
6. Terry G, Ho L, Londesborough P, Duggan C, Hanby A, Cuzick J. The expression of FHIT, PCNA and EGFR in benign and malignant breast lesions. Br J Cancer 2007;96(1):110-117.
7. Greenspan DL, Connolly DC, Wu R, Lei RY, Vogelstein JTC, Kim YT, et al. Loss of FHIT expression in cervical carcinoma cell lines and primary tumors. Cancer Res 1997;57(21):4692-4698.
8. Cao J, Li W, Xie J, Du H, Tang W, Wang H, et al. Down-regulation of FHIT inhibits apoptosis of colorectal cancer: mechanism and clinical implication. Surg Oncol 2006;15(4):223-233.
9. Moore CD, Shahrokh K, Sontum SF, Cheatham TE, Yost GS. Improved cytochrome P450 3A4 molecular models accurately predict the Phe215 requirement for raloxifene dehydrogenation selectivity. Biochemistry 2010;49(41):9011-9019.
10. Ding Y, Larson G, Rivas G, Lundberg C, Geller L, Ouyang C, et al. S Strong signature of natural selection within an FHIT intron implicated in prostate cancer risk. Plos One 2008;3(10):e3533.
11. Ohta M, Inoue H, Cotticelli MG, Kastury K, Baffa R, Palazzo J, et al. The FHIT gene, spanning the chromosome 3p14.2 fragile site and renal carcinoma-associated t(3;8) breakpoint, is abnormal in digestive tract cancers. Cell 1996;84(4):587-597.
12. Baffa R, Veronese ML, Santoro R, Mandes B, Palazzo JP, Rugge M, et al. Loss of FHIT expression in gastric carcinoma. Cancer Res 1998;58(20): 4708-4714.
13. Perez-Ordonez B, Beauchemin M, Jordan RCK. Molecular biology of squamous cell carcinoma of

the head and neck. J Clin Pathol 2006;59(5):445-453.

14. Nishizaki M, Sasaki J, Fang B, Atkinson EN, Minna JD, Roth JA, et al. Synergistic tumor suppression by coexpression of FHIT and p53 coincides with FHIT-mediated MDM2 inactivation and p53 stabilization in human non-small cell lung cancer cells. Cancer Res 2004;64(16):5745-5752.
15. Orengo CA, Thornton JM. Alpha plus beta folds revisited: some favoured motifs. Structure 1993;1 (2):105-120.
16. Lima CD, D Amico KL, Naday I, Rosenbaum G, Westbrook EM, Hendrickson WA. MAD analysis of FHIT, a putative human tumor suppressor from the HIT protein family. Structure 1997;5(6):763-774.
17. Freedman DA, Epstein CB, Roth JC, Levine AJ. A genetic approach to mapping the p53 binding site in the MDM2 protein. Mol Med 1997;3(4):248-259.
18. Freedman DA, Levine AJ. Regulation of the p53 protein by the MDM2 oncoprotein-thirty-eighth G.H.A. Clowes Memorial Award Lecture. Cancer Res 1999;59(1):1-7.
19. Cavazzoni A, Galetti M, Fumarola C, Alfieri RR, Roz L, Andriani F, et al. Effect of inducible FHIT and p53 expression in the Calu-1 lung cancer cell line. Cancer Lett 2007;246(1-2):69-81.
20. Fan H, Wang X, Zhu J, Robillard GT, Mark AE. Molecular dynamics simulations of the hydrophobin SC3 at a hydrophobic/hydrophilic interface. Proteins 2006;64(4):863-873.
21. Eswar N, Webb B, Marti-Renom MA, Madhusudhan MS, Eramian D, Shen MY, et al. Comparative protein structure modeling using MODELLER. Curr Protoc Protein Sci 2007;Chapter 2:Unit 2.9.
22. Fahham N, Ghahremani MH, Sardari S, Vaziri B, Ostad SN. Simulation of different truncated p16 (INK4a) forms and in silico study of interaction with Cdk4. Cancer Inform 2009;7:1-11.
23. Ritchie DW, Kemp GJ. Protein docking using spherical polar fourier correlations. Proteins 2000; 39(2):178-194.
24. Ritchie DW. Evaluation of protein docking predictions using Hex 3.1 in CAPRI rounds 1 and 2. Proteins 2003;52(1):98-106.
25. Oliner JD, Pietenpol JA, Thiagalingam S, Gyuris J, Kinzler KW, Vogelstein B. Oncoprotein MDM2 conceals the activation domain of tumour suppressor p53. Nature 1993;362(6423):857-860.
26. Chen J, Marechal V, Levine AJ. Mapping of the p53 and mdm-2 interaction domains. Mol Cell Biol 1993;13(7):4107-4114.
27. Lin J, Chen J, Elenbaas B, Levine AJ. Several hydrophobic amino acids in the p53 amino-terminal domain are required for transcriptional activation, binding to mdm-2 and the adenovirus 5 E1B 55-kD protein. Genes Dev 1994;8(10):1235-1246.
28. Zhao Y, Bernard D, Wang S. Small molecule inhibitors of MDM2-p53 and MDMX-p53 interaction as new cancer therapeutics. BioDiscovery 2013;4 (8):1-15.
29. Chene P. Inhibition of the p53-MDM2 interaction: targeting a protein-protein interface. Mol Cancer Res 2004;2(1):20-28.
30. Vassilev LT, Vu BT, Graves B, Carvajal D, Podlaski F, Filipovic Z, et al. In vivo activation of the p53 pathway by small-molecule antagonists of MDM2. Science 2004;303(5659):844-848.
31. Fuchs SY, Adler V, Buschmann T, Wu X, Ronai Z. Mdm2 association with p53 targets its ubiquitination. Oncogene 1998;17(19):2543-2547.
32. Michael D, Oren M. The p53-Mdm2 module and the ubiquitin system. Semin Cancer Biol 2003;13 (1):49-58.
33. Moll UM, Petrenko O. The MDM2-p53 interaction. Mol Cancer Res 2003;1(14):1001-1008.
34. Bahnassy AA, Zekri AR, Madbouly MS, El-Naggar M, El-Khelany ZF, El-Merzebany MM. The correlation between FHIT, P53 and MMR genes in human papillomavirus-associated cervical carcinoma. J Egypt Natl Canc Inst 2006;18(3):191-202.
35. Grasberger BL, Lu T, Schubert C, Parks DJ, Carver TE, Koblish HK, et al. Discovery and cocrystal structure of benzodiazepinedione HDM2 antagonists that activate p53 in cells. J Med Chem 2005; 48(4):909-912.